AGU PUBLICATIONS

JGR

Journal of Geophysical Research: Space Physics

RESEARCH ARTICLE

10.1002/2014JA020631

Key Points:
- We produce a superposed epoch analysis of substorms, SEs, and SMCs
- SMCs with substorms during the 2 h before onset are part of substorm cycle
- SMCs with associated substorms occur during the expansion phase of substorms

Correspondence to:
M.-T. Walach,
mw309@le.ac.uk

Citation:
Walach, M.-T., and S. E. Milan (2015), Are steady magnetospheric convection events prolonged substorms?, *J. Geophys. Res. Space Physics*, *120*, 1751–1758, doi:10.1002/2014JA020631.

Received 18 SEP 2014
Accepted 9 FEB 2015
Accepted article online 12 FEB 2015
Published online 12 MAR 2015

Are steady magnetospheric convection events prolonged substorms?

M.-T. Walach[1] and S. E. Milan[1]

[1]Department of Physics and Astronomy, University of Leicester, Leicester, UK

Abstract Magnetospheric modes, including substorms, sawtooth events, and steady magnetospheric convection events, have in the past been described as different responses of the magnetosphere to coupling with the solar wind. Using previously determined event lists for sawtooth events, steady magnetospheric convection events, and substorms, we produce a statistical study of these event types to examine their similarities and behavior in terms of solar wind parameters, auroral brightness, open magnetospheric flux, and geomagnetic indices. A superposed epoch analysis shows that individual sawteeth show the same signatures as substorms but occur during more extreme cases of solar wind driving as well as geomagnetic activity. We also explore the limitations of current methods of identifying steady magnetospheric convection events and explain why some of those events are flagged inappropriately. We show that 58% of the steady magnetospheric convection events considered, as identified by criteria defined in previous studies are part of a prolonged version of substorms due to continued dayside driving during expansion phase. The remaining 42% are episodes of enhanced magnetospheric convection, occurring after extended periods of dayside driving.

1. Introduction

The dynamics of the Earth's magnetosphere are driven largely by its interaction with the solar wind. Magnetic reconnection between the interplanetary magnetic field (IMF) and the terrestrial dipole occurring near the subsolar magnetopause produces an accumulation of open flux in the magnetotail lobes, which can be observed as a growth of the polar cap [*Cowley and Lockwood*, 1992; *Milan et al.*, 2012]. Eventually the magnetosphere must reclose this flux by magnetic reconnection in the magnetotail, though this response can be delayed, episodic, or prolonged [*Pulkkinen et al.*, 2007].

Different types of responses have been termed "magnetospheric modes" in the past. Examples of these modes are substorms, steady magnetospheric convection (SMC) events, and sawtooth events (SEs), which are the focus of this study [e.g., *Pulkkinen et al.*, 2010; *Partamies and Pulkkinen*, 2009; *DeJong et al.*, 2009; *Huang et al.*, 2009; *McPherron et al.*, 2008].

Substorms are explosive unloading events, which follow a period of open flux accumulation known as the growth phase [*Baker et al.*, 1996]. At onset, the polar cap decreases in size as nightside reconnection dominates over dayside reconnection [*Milan et al.*, 2007, 2009]. This makes substorms an example of an event where the nightside flux closure response is delayed with respect to the loading phase. SMCs, on the other hand, are said to be periods where enhanced, quasi-steady convection dominates magnetospheric activity [*Sergeev et al.*, 1996], as the dayside and nightside reconnection rates are balanced, such that the open flux stays approximately constant. Hence, these have also been called "balanced reconnection intervals" [*DeJong et al.*, 2008]. SEs are sequences of quasiperiodic energetic unloadings named after their characteristic signatures in energetic particle fluxes detected at geosynchronous orbit [*Belian et al.*, 1995]. SEs have often been likened to intense substorms as they have many features in common, for example, the development of the DP-1 current pattern [*Cai et al.*, 2006]. The magnetospheric flux closure associated with SEs is thus said to be episodic due to the quasiperiodic nature of the measured sawtooth signatures.

A relation between substorms and SMC occurrences has been shown in the past. *Sergeev et al.* [1996], for example, noted that all SMCs either start or end with a substorm. They concluded that SMCs either are just an active period between substorms or can only occur following a substorm. *McPherron et al.* [2005] showed a similar relationship between substorms and SMCs and suggested that substorms are necessary for the termination of SMC events. *Kissinger et al.* [2012] supported the findings of *Sergeev et al.* [1996], as they

showed that most SMCs follow substorm-like signatures and only 1% of SMCs are initiated without much preceding magnetospheric activity.

We use event lists compiled by previous workers to identify periods undergoing different magnetospheric modes. First, we describe the event lists and data sets that we bring to our analysis, and then we outline how we combine these lists and remove ambiguous events. We perform a large-scale statistical analysis in the form of superposed epoch analysis of substorms, SMCs, and SEs to identify how they behave in terms of open magnetospheric flux and other measures of magnetospheric activity.

2. Data and Data Reduction

For the SE we use two event lists: one produced by *Cai et al.* [2006] and the other by Henderson and McPherron [see *Pulkkinen et al.*, 2007]. Both examined energetic particle fluxes at geosynchronous orbit to identify the characteristic sawtooth signature of sharp enhancements followed by gradual decreases. Their criteria were that there had to be a series of quasiperiodic sawteeth in the data and that they had to be observed by at least two spacecraft, one near local noon and the other near midnight (± 3 h magnetic local time).

The substorm list we utilize was compiled by *Frey et al.* [2004], who used observations from the far ultraviolet (FUV) imager instrument suite [*Mende et al.*, 2000a, 2000b] onboard the Imager for Magnetopause-to-Aurora Global Exploration (IMAGE) satellite [*Burch*, 2000] to identify the onset of auroral brightenings associated with substorms.

The SMCs we use were identified by *Kissinger et al.* [2011], who studied the electrojet indices *AL* and *AU* as a proxy for magnetospheric convection. The SMC list included start and end times of each event, whereas the substorm and SE lists included onset only.

We supplement these lists with observations of the auroras from the IMAGE satellite taken with the Wideband Imaging Camera (WIC) and Spectrographic Imager (SI12) instruments, part of the FUV suite, which primarily measure electron and proton aurorae, respectively, at a cadence of approximately 2 min. Data coverage from IMAGE was not continuous with there being a data gap of approximately 4 h every 13 h orbit. As reported by *Shukhtina and Milan* [2014], these images have been processed to extract integrated brightness, as well as an estimate of the open magnetic flux content of the magnetosphere, F_{PC}, using the size of the polar cap as a proxy. To estimate the open-closed field line boundary, the poleward edge of the auroral oval was used as a proxy, as described by *Shukhtina and Milan* [2014]. IMAGE data are only available for the period of May 2000 to October 2005, and this defines the interval considered by our study.

In conjunction with these data sets we have used 1 min OMNI (Operating Missions as a Node on the Internet) data for solar wind parameters (solar wind speed, V_{SW}, and the interplanetary magnetic field components, B_X, B_Y, and B_Z), as well as data for the *SYM-H*, *AU*, and *AL* indices downloaded from NASA's CDAweb (see http://omniweb.gsfc.nasa.gov/html/HROdocum.html for more information). The solar wind parameters are used to estimate the dayside reconnection rate, Φ_D, based on the formulation of *Milan et al.* [2012].

Simply using the aforementioned event lists by themselves is problematic. For example, SEs are known to be characteristically similar to substorms, and as a result, SEs have been described as substorms before [e.g., *Henderson*, 2004]. There is some overlap in our lists with *Frey et al.* [2004] having identified all brightenings as substorms; we remove all substorms from the list that are also classified as an SE (±15 min of onset). Similarly, only using auroral electrojet index thresholds are not necessarily a reliable indicator of steady magnetospheric convection as shown by *McWilliams et al.* [2008].

In order to avoid ambiguities between event types, the event lists were examined for inconsistencies. We studied each SMC event individually to ensure that they fitted the physical criteria for balanced reconnection interval as described by *DeJong et al.* [2009, 2008]. For all SMC, where more than 50% of the event interval had corresponding IMAGE data available (391 events), we examined F_{PC}, WIC brightness, *AU*, *AL*, IMF B_z (in GSM coordinates), and Φ_D to manually deselect SMC events that are either not steady (F_{PC} and WIC brightness show substorm signatures) or not convective (Φ_D is below 20 kV for most of the event). SMCs where less than 50% of the data from IMAGE were unavailable were also deselected.

An example SMC event is shown in Figure 1 to illustrate why some events were rejected. Figure 1 shows F_{PC}, *AL* and *AU*, maximum auroral intensity as measured by WIC, IMF B_z, and Φ_D during an event identified

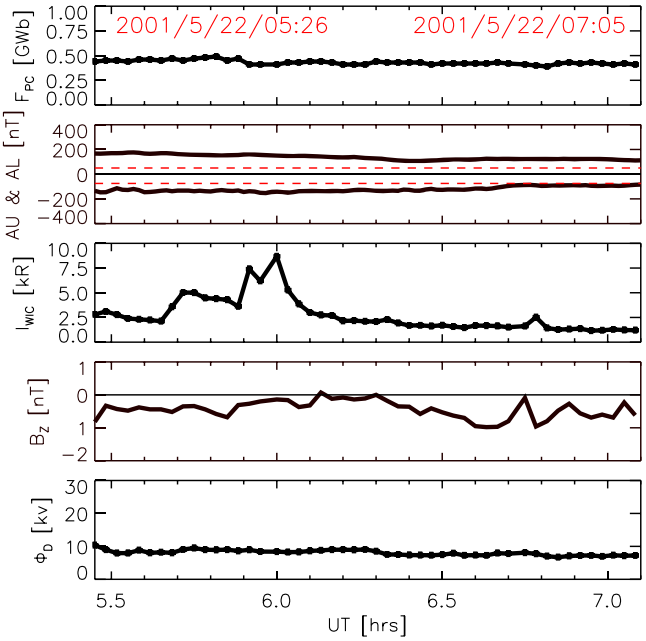

Figure 1. Example SMC event, showing F_{PC}, *AU* and *AL*, auroral brightness as measured by WIC, IMF B_z, and Φ_D. The dashed lines in the *AU* and *AL* plots indicate the thresholds as set out by *Kissinger et al.* [2011] criteria. The data derived from IMAGE measurements are plotted as crosses, joined up by lines to indicate the data density.

by *Kissinger et al.* [2011]. We see that although F_{PC} stays fairly constant over the event, which could indicate the occurrence of an SMC, Φ_D is below ~20 kV for the duration of the interval, indicating that there is insignificant convection within the magnetosphere, which is why the event was deselected. We also plot the WIC brightness, which was used in some cases to help identify substorms, but the brightness peak in this case was not used as such an identifier, as there are no changes in F_{PC} occurring at that time.

Figure 2 shows the substorm occurrences in relation to the SMCs' onset and ending of events. As all SMCs have differing event lengths, each SMC's event duration was normalized, such that we can consider the event timings in terms of percentage of event, with 0% at the start and 100% at the end. The occurrences of substorms were then binned with a bin length of 10% of SMC event length. We also plotted the occurrences of substorms previous and subsequent to SMCs. The average duration of the SMC events was just less than 200 min. The grey histogram has been calculated using the original SMC list, whereas the blue histogram only uses the manually selected SMCs. Both occurrence distributions show peaks just before and just after the SMC events start and end. Figure 2 also shows that some of the *Frey et al.* [2004] substorms occur during the SMCs, but the number of these events is relatively small. These substorms are pseudobreakups and similar brightenings, as we checked for substorm onsets during every SMC (plotted as in Figure 1) and deselected all SMCs with substorms occurring. As a result of the large number of substorm events occurring during the time leading up to the SMCs, we further subdivided the SMC list: for all the SMCs, which have a substorm occurring during the 2 h preceding the SMC interval, the SMC event is retimed, such that the beginning of the event is shifted to match the closest substorm onset. For all other SMCs the onset and end times are kept the same. Refining the start of SMCs preceded by substorms allows us to study the evolution of magnetospheric behavior from the initiating substorm into the following SMC.

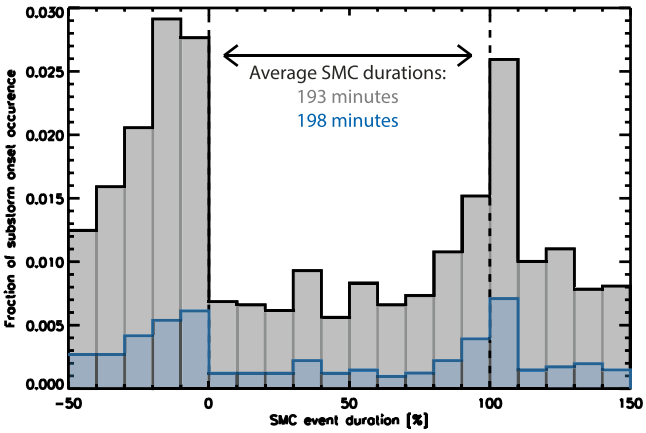

Figure 2. Occurrence distribution of substorms with respect to the onset and the end of SMCs. The number of substorms per bin are normalized by the total number of substorms considered (4083 substorms). The black histogram shows the substorms in relation to the original SMC list, and the blue histogram shows the substorm occurrence in relation to the manually selected SMC list.

DeJong et al. [2007] and *Huang et al.* [2009] composed superposed epoch analysis of the F_{PC} for SEs, SMCs, and substorms, but our analysis completes this study because we use a much larger data set. *DeJong et al.* [2007] used only 45 SMCs, 29 SEs, and 31 isolated substorms, whereas we use 4083 substorms, 273 SEs, 154 SMCs

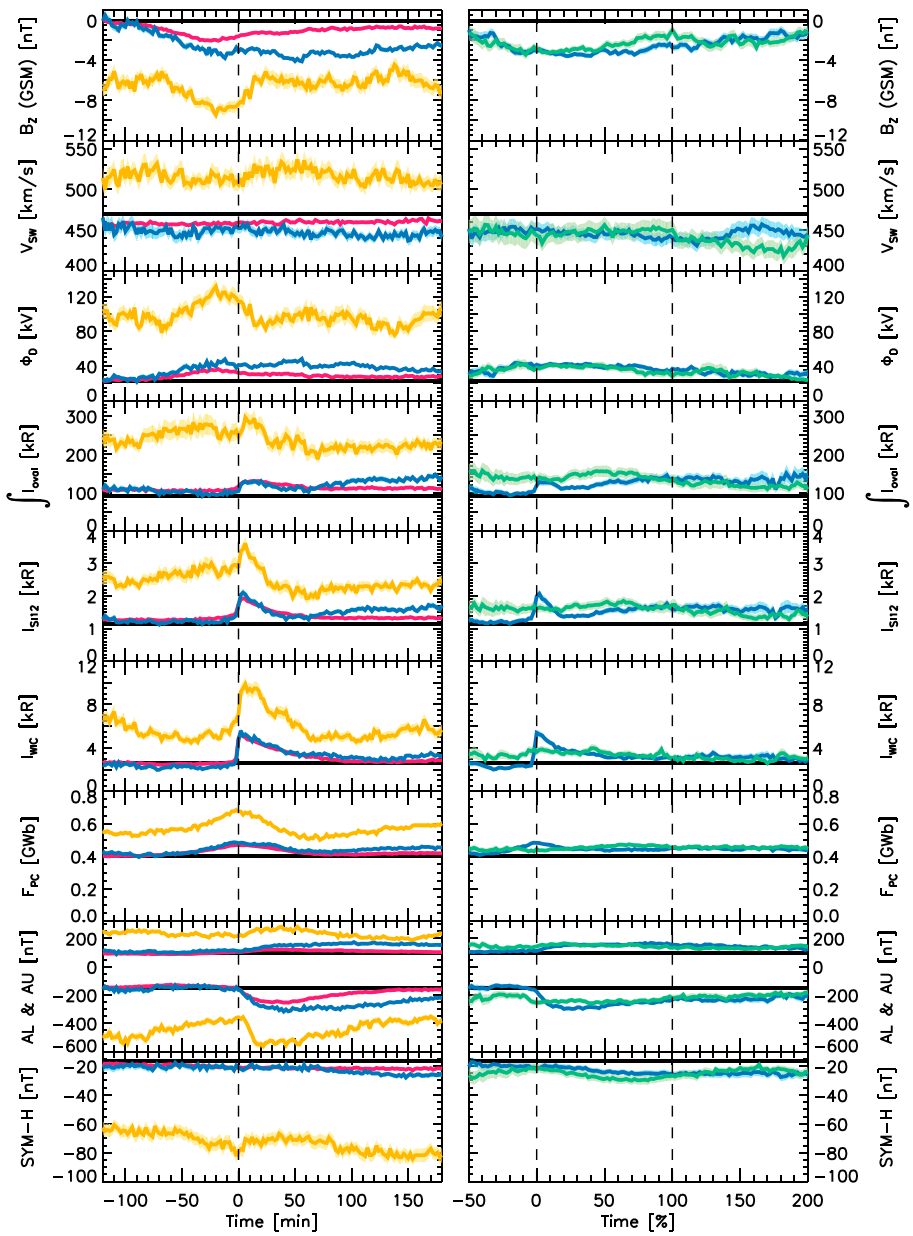

Figure 3. Plots showing a superposed epoch analysis of substorms (red), SEs (orange), and SMCs (blue and green). The paler areas indicate the size of the standard errors on the mean. The averages for the whole data set are shown by the black horizontal lines, and zero epochs are indicated by the dashed lines. The blue lines show the mean of the SMCs that have a preceding substorm and the onset of those events has been shifted to the onset of the substorms, whereas the green SMCs are the remaining SMCs with no preceding substorm. The onset is zero epoch (left column) and a timescale normalized to event duration (right column). The green SMCs have been omitted from Figure 3 (left column) for clarity. The rows show the superposed epoch analysis of the IMF B_Z component, the solar wind speed, Φ_D, integrated oval intensity, maximum oval intensity as measured by the SI12 and WIC instruments, F_{PC}, *AL* and *AU*, and *SYM-H*.

with preceding substorms, and 113 SMCs without preceding substorms. We also look at the superposed epoch analysis using the end time of the SMCs as zero epoch to establish how the SMCs conclude.

3. Observations

Figure 3 shows a series of superposed epoch analysis for the substorms, SMCs, and SEs. The substorms are shown in red, the SEs in orange, and the SMCs in green and blue. The blue SMCs have preceding substorms during the 2 h beforehand, and their zero epoch has been shifted to match the substorm onset, whereas the

green SMCs do not have preceding substorms. The paler areas indicate the sizes of the standard errors on the means, and the zero epochs are shown by the dashed lines. The horizontal black lines show the averages for each parameter for the whole period from May 2000 to October 2005. For Figure 3 (left column), onset was taken as the zero epoch, and the superposed epoch analysis were calculated with a cadence of 2 min. Figure 3 (right column) shows superposed epoch analysis where the timescales have been stretched, relative to the start and end times of the SMCs, the data were binned and averaged at a cadence of 2% of the event duration.

The signatures of the substorms in Figure 3 show a decrease in the IMF B_Z component, becoming clearly southward prior to their onset, peaking about 25 min before onset, which is followed by a gradual recovery toward 0 nT. We plot B_Z along with V_{SW} as the only solar wind parameters, as they directly modulate Φ_D and with it the magnetospheric dynamics. V_{SW} shows no particular characteristics for substorms. Φ_D thus mirrors the behavior of B_Z, so the substorm average increases before onset, reaching a maximum at $T = -25$ min and then decreases again, all beginning and ending near the global mean. The integrated emission intensity of the auroral oval has values near the global mean at the beginning and increases sharply at onset, as expected due to Frey's selection criteria. The integrated intensity for the substorms then stays elevated for an hour or so before decreasing again. The maximum intensity given by the SI12 and WIC instruments onboard IMAGE shows similar patterns to the integrated brightness for the substorms: we see a sharp increase at onset, followed by a gradual decrease during the substorm toward normal values. The polar cap flux for the substorms is near the average value, 0.4 GWb, at the beginning of the interval shown, and increases to 0.5 GWb at onset. F_{PC} then decreases again to its starting point. The *AU* index for substorms is slightly below the average for the data set and increases to values slightly above it at onset, whereas the *AL* index starts off above the average and shows a clear decrease, commencing at onset, which is followed by a gradual increase. The *SYM-H* index for the substorms is near the average and shows a very gradual decreasing trend over the period shown.

In almost all respects, the blue SMC traces, which are initiated by substorms, follow those of the substorms up to and including onset. Thereafter, the substorm traces subside toward average values, whereas the SMC traces remain elevated; that is, B_Z remains uniformly southward, F_{PC} and Φ_D remain enhanced above the average, the aurorae remain bright, and the *AU* and *AL* indices remain elevated.

Green SMCs, which are not initiated by a substorm, show similarities and differences to blue SMCs. B_Z remains negative for the duration of the events, and *AL* and *AU* are elevated. However, green SMCs do not show an abrupt onset in *AL* or auroral intensity as they do not begin with substorms. The main difference is in *SYM-H*, which is more negative than the blue trace at $T = -50\%$; then the green trace increases slowly until onset, when it becomes more negative again.

The SE signatures in Figure 3 are very similar to substorms, as they show the same variations, though significantly more enhanced. The only one that does not show the same signature is the integrated auroral oval intensity, which shows that the aurorae are on average approximately twice as bright prior to SE compared to just before substorm onset. The SE do show an overall increase in oval intensity, but the onset is not as clearly defined as for substorm onsets.

4. Discussion

Out of the 391 SMC events where IMAGE data are of good quality (see *Shukhtina and Milan* [2014] for definition), we rejected 32% of events as either Φ_D was close to zero for most of the event or F_{PC} was too variable. This illustrates how problematic it is to just use *AU* and *AL* as proxies for magnetospheric convection. Two hundred twenty-nine SMCs were considered and subdivided into two categories: events where substorms occurred during the 2 h preceding the SMC and events where no substorm occurred before SMC onset. The SMCs with preceding substorms were retimed, such that the SMC onset matches substorm onset.

The superposed epoch analysis for the substorms show very distinct features just before or at onset, followed by gradual recoveries: prior to onset the dayside reconnection rate reaches a maximum, as B_Z is most southward approximately half an hour before onset; the intensity of the aurorae peak at onset, as well as the open magnetospheric flux; *AL* decreases sharply at onset to reach a minimum after onset. These signatures are well known for substorms, where a period of southward IMF leads to magnetopause

reconnection, such that the accumulation of newly open magnetic flux in the lobes forces the polar cap to expand, and *AL* and *AU* enhance as convection is excited. At some point reconnection in the magnetotail is initiated, leading to auroral brightenings and the formation of the substorm current wedge and thus the characteristic substorm bay in *AL*. The trend of a decrease in the magnitude of B_Z prior to substorm onset has been widely reported, as well as the suggestion that substorms are triggered by a northward turning of the IMF [e.g., *Caan et al.*, 1977; *Lyons*, 1995]. This was disputed by *Morley and Freeman* [2007], *Freeman and Morley* [2004, 2009], and *Wild et al.* [2009] (among others) to be as a consequence of the natural variability of the IMF and the fact that close to substorm onset, it is no longer required that the growth phase continue for the substorm to be initiated.

Approximately 58% of all SMCs we examined have a substorm occurring during the 2 h preceding the SMC onset. If we consider this to be the onset of an event, we see almost identical signatures to substorms following the pre-SMC substorm onset. The introduced time shift makes it possible to see the substorm at the onset, as well as the following SMC. The difference between these SMCs and substorms is that the IMF remains southward beyond the time of onset and magnetopause reconnection continues into the expansion phase, when magnetotail reconnection has also commenced.

This means that the polar cap contracts slower than it usually does for substorms after onset; it continues to be enlarged for longer and the open flux content of the magnetosphere stays approximately constant throughout the event. The IMF B_Z component will gradually turn more northward toward the event conclusion and the SMC will end at some point during this transition. At this point, the dayside reconnection decreases but the magnetotail continues into a "recovery phase" as F_{PC} continues to decrease very gradually for several hours (not shown on this time scale). The intensity of the aurorae, as well as *AL* will decrease at this time. A decrease in the southward component of the IMF can be seen in the blue trace in Figure 3 toward the conclusion of these SMCs, at approximately $T = 60\%$.

DeJong et al. [2008] showed an example of an SMC event in their study that appears similar to our substorm-following SMCs: a substorm initiates nightside reconnection, but F_{PC} remains enhanced and steady, along with the auroral brightness during their event. The end of the auroral activity is marked in their event by B_Z becoming more northward. Their data suggest that the extended southward component of the IMF and its gradual northward turning allows the reconnection rates to continue to be enhanced and balanced while the magnetotail is relaxing back to a quiet state. Our substorm-following SMCs progress in a similar manner, and we can see clearly that it is the substorm onset that initiates the necessary flux closure. Our event is not strictly a driven recovery phase, but rather a driven expansion phase, as flux continues to be closed after the SMC has concluded. It is hard to distinguish where the event phases start and end in our superposed epoch analysis, so the SMC may be part of the expansion or early recovery phase. We do know, however, that the recovery phase continues after the SMC as the auroral brightness continues to decrease, as well as the dayside reconnection rate and the open flux, and thus, the magnetosphere is still relaxing after the SMC event has ended.

In the past, researchers [e.g., *McPherron et al.*, 2005; *DeJong et al.*, 2009; *Kissinger et al.*, 2011, 2012] thought that the event-preceding substorms are necessary for SMCs to occur and precondition the magnetosphere in some way, whereas we show that approximately half of SMCs are part of the substorm cycle. We would reclassify "classic" substorms as those which coincidentally have a decrease in Φ_D, following the clear enhancement prior to onset, whereas "substorms + SMCs" events are those for which Φ_D remains elevated after onset. This naturally explains the debate regarding the occurrence of northward turnings for triggering substorms: those that do not have a northward turning or rather a reduction in the southward component do not look like classic substorms and develop into SMCs instead.

Sergeev et al. [1996] suggest that it is necessary for SMCs to have a preceding substorm as the magnetosphere needs this release of flux in order to be able to reach a quasi-steady state, as their data suggest that SMCs are an active period between substorms. The percentage of events with preceding substorms in our study is considerably lower than theirs, suggesting that the substorms may not be necessary for the establishment of steady convection. Our superposed epoch analysis shows that the SMCs with preceding substorms are part of the evolution of the substorm event.

The rest of the SMCs (42% of all considered events) do not share exactly the same characteristics as the substorm preceded SMCs; instead, the aurorae are intensified before onset, as well as the *AL* index and

continue to be throughout the events. The *SYM-H* index indicates more disturbed geomagnetic conditions, but most significantly, the dayside driving is much more prolonged than for the SMCs with preceding substorms (not shown on the timescales of Figure 3). These SMCs show a long stretch of southward IMF, which starts approximately 13 h before onset, whereas substorms preceding SMCs only show a southward IMF leading up to the event as the substorm growth phase occurs (shown in Figure 3). We speculate that the magnetosphere needs either this prolonged dayside driving for steady convection to occur or a substorm to help initiate the flux closure.

Similar to our study, *Kissinger et al.* [2012] found that 92% of all SMCs occur within 75 min of a substorm onset. Although they use the same SMC criteria, their fraction of events with or without preceding substorms differs to ours because they do not exclude events where no dayside driving occurs. Although they find that 1% of SMCs occur after a quiet magnetosphere and the remaining events after substorm-like behavior, we speculate that their 1% belongs to the events we have excluded due to insufficient dayside driving.

O'Brien et al. [2002] show that for SMCs to occur, V_{SW} values below 450 km/s are preferential; our data agrees with this. For all of the events, except SEs, V_{SW} stays just below the average for the whole data set, which is around 470 km/s. For SEs, the V_{SW} average stays at or above 500 km/s. This indicates that fast solar wind speeds are not necessarily needed for active periods in the magnetosphere.

In their studies of SEs, SMCs, and substorms, *DeJong et al.* [2007] and *Huang et al.* [2009] showed that on average, F_{PC} for SE reaches at least 1 GWb before onset. Our data set, however, barely ever reaches such high values, so the average F_{PC} for SE at onset is just below 0.7 GWb. Our superposed epoch analysis agree with those of *DeJong et al.* [2007] and *Huang et al.* [2009] in terms of the overall shape of F_{PC}, the values, however, differ. This is most likely due to a systematic offset brought about by different F_{PC} estimation methods. Our interpretation, in line with that of *DeJong et al.* [2007] and *Huang et al.* [2009], is that SEs show all the characteristics of substorms occurring during disturbed geomagnetic conditions, storm conditions even, and strong solar wind driving. Due to our larger selection of events, we can now be more certain of these characteristic condition within SEs occur.

5. Summary and Conclusions

Approximately 58% of all SMCs considered have a substorms occurring in the 2 h before onset. These events show signatures just like substorms with the expansion phase stretched over a longer time span. We conclude that the majority of SMCs flagged by the *Kissinger et al.* [2011] selection criteria are driven expansion or recovery phases of substorms, which show an increase of the polar cap flux before onset. During the event itself, the prolonged enhanced dayside reconnection rate is continually driving the convection, unlike for substorms, during which the dayside driving is lower and does not dominate throughout the event. This means that the polar cap cannot contract, and we see elevated auroral intensities throughout the event. *AL* and *AU* remain elevated throughout this period, as given by the definition of an SMC by the *Kissinger et al.* [2011] criteria. The recovery phase commences when the dayside driving decreases and polar cap flux decreases, and thus, the substorm recovery continues after the SMC has concluded. Around 42% of the SMCs do not have substorms occurring during the 2 h previous to the events and occur after prolonged dayside driving (approximately 13 h thereof). Similarly, SEs occur during enhanced geomagnetic activity and convection. They show the same signatures as substorms, but the characteristics are more enhanced and extreme. Most significantly, the magnetospheric response is qualitatively the same for substorms and SEs in terms of flux closure, although on a differing scale. We conclude with the notion that the majority of SMCs, as they have been selected in the past, are part of the substorm process and could also be considered driven expansion or driven recovery phase due to continued dayside driving.

Acknowledgments

We are grateful to the PI of IMAGE, J.L. Burch, and the PI of FUV, S.B. Mende, for the original IMAGE data set. The OMNI data are provided by the GSFC/SPDF OMNIWeb platform, and we are grateful to the PIs of the data set used: J.H. King and N. Papitashvili. We thank J. Kissinger, H. Frey, X. Cai, M. Henderson, and R. McPherron for the provision of the event lists. The IMAGE processing was supported by the European Union Framework 7 Programme, ECLAT Project grant 263325. M.-T.W. was supported by a studentship from the Science and Technology Facilities Council, UK. S.E.M. was supported on the STFC grant ST/K001000/1. The authors would also like to thank T. K. Yeoman for his helpful input. The OMNI data used in this study are available on the GSFC/SPDF OMNIWeb platform, which can be found at http://cdaweb.gsfc.nasa.gov/. The original IMAGE data are available through the IMAGE FUV homepage (http://sprg.ssl.berkeley.edu/image/), and the analyzed IMAGE data set is available from the Cluster Science Archive (http://www.cosmos.esa.int/web/csa/). The event lists and code used to generate the plots in this paper are stored on University of Leicester computers and are available on request.

Larry Kepko thanks Kathryn McWilliams and another reviewer for their assistance in evaluating this paper.

References

Baker, D. N., T. I. Pulkkinen, V. Angelopoulos, W. Baumjohann, and R. L. McPherron (1996), Neutral line model of substorms: Past results and present view, *J. Geophys. Res.*, *101*(A6), 12,975–13,010.

Belian, R. D., T. E. Cayton, and G. D. Reeves (1995), Quasi-periodic global substorm generated flux variations observed at geosynchronous orbit, in *Space Plasma: Coupling Between Small and Medium Scale Processes, Geophys. Monogr. Ser.*, vol. 86, edited by M. Ashour-Abdalla, T. Chang, and P. Dusenbery, pp. 143–148, AGU, Washington, D. C., doi:10.1029/GM086p0143.

Burch, J. L. (2000), IMAGE mission overview, *Space Sci. Rev.*, *91*, 1–14.

Caan, M. N., R. L. McPherron, and C. T. Russell (1977), Characteristics of the association between the interplanetary magnetic field and substorms, *J. Geophys. Res.*, *82*(29), 4837–4842, doi:10.1029/JA082i029p04837.

Cai, X., C. R. Clauer, and A. J. Ridley (2006), Statistical analysis of ionospheric potential patterns for isolated substorms and sawtooth events, *Ann. Geophys.*, *24*, 1977–1991.
Cowley, S. W. H., and M. Lockwood (1992), Excitation and decay of solar wind-driven flows in the magnetosphere-ionophere system, *Ann. Geophys.*, *10*, 103–115.
DeJong, A. D., X. Cai, C. R. Clauer, and J. F. Spann (2007), Aurora and open magnetic flux during isolated substorms, sawteeth, and SMC events, *Ann. Geophys.*, *25*, 1865–1876.
DeJong, A. D., A. J. Ridley, and C. R. Clauer (2008), Balanced reconnection intervals: Four case studies, *Ann. Geophys.*, *26*, 3897–3912.
DeJong, A. D., A. J. Ridley, X. Cai, and C. R. Clauer (2009), A statistical study of BRIs (SMCs), isolated substorms, and individual sawtooth injections, *J. Geophys. Res.*, *114*, A08215, doi:10.1029/2008JA013870.
Freeman, M. P., and S. K. Morley (2004), A minimal substorm model that explains the observed statistical distribution of times between substorms, *Geophys. Res. Lett.*, *31*, L12807, doi:10.1029/2004GL019989.
Freeman, M. P., and S. K. Morley (2009), No evidence for externally triggered substorms based on superposed epoch analysis of IMF Bz, *Geophys. Res. Lett.*, *36*, L21101, doi:10.1029/2009GL040621.
Frey, H. U., S. B. Mende, V. Angelopoulos, and E. F. Donovan (2004), Substorm onset observations by IMAGE-FUV, *J. Geophys. Res.*, *109*, A10304, doi:10.1029/2004JA010607.
Henderson, M. G. (2004), The May 2–3, 1986 CDAW-9C interval: A sawtooth event, *Geophys. Res. Lett.*, *31*, L11804, doi:10.1029/2004GL019941.
Huang, C.-S., A. D. DeJong, and X. Cai (2009), Magnetic flux in the magnetotail and polar cap during sawteeth, isolated substorms, and steady magnetospheric convection events, *J. Geophys. Res.*, *114*, A07202, doi:10.1029/2009JA014232.
Kissinger, J. E., R. L. McPherron, T.-S. Hsu, and V. Angelopoulos (2011), Steady magnetospheric convection and stream interfaces: Relationship over a solar cycle, *J. Geophys. Res.*, *116*, A00I19, doi:10.1029/2010JA015763.
Kissinger, J. E., R. L. McPherron, T.-S. Hsu, V. Angelopoulos, and X. Chu (2012), Necessity of substorm expansions in the initiation of steady magnetospheric convection, *Geophys. Res. Lett.*, *39*, L15105, doi:10.1029/2012GL052599.
Lyons, L. R. (1995), A new theory for magnetospheric substorms, *J. Geophys. Res.*, *100*(A10), 19,069–19,081, doi:10.1029/95JA01344.
McPherron, R. L., T. P. O'Brien, and S. Thompson (2005), Solar wind drivers for steady magnetospheric convection, in *Multiscale Coupling of Sun-Earth Processes,* chap. 2: Space Storms, edited by A. T. Y. Lui, Y. Kamide, and G. Consolini, pp. 113–124, Elsevier Science B. V., Amsterdam.
McPherron, R. L., J. M. Weygand, and T.-S. Hsu (2008), Response of the Earth's magnetosphere to changes in the solar wind, *J. Atmos. Sol. Terr. Phys.*, *70*(2–4), 303–315, doi:10.1016/j.jastp.2007.08.040.
McWilliams, K. A., J. B. Pfeifer, and R. L. McPherron (2008), Steady magnetospheric convection selection criteria: Implications of global SuperDARN convection measurements, *Geophys. Res. Lett.*, *35*, L09102, doi:10.1029/2008GL033671.
Mende, S. B., et al. (2000a), Far ultraviolet imaging from the IMAGE spacecraft: 1. System design, *Space Sci. Rev.*, *91*, 243–270.
Mende, S. B., et al. (2000b), Far ultraviolet imaging from the IMAGE spacecraft: 2. Wideband FUV imaging, *Space Sci. Rev.*, *91*, 271–285.
Milan, S. E., G. Provan, and B. Hubert (2007), Magnetic flux transport in the Dungey cycle: A survey of dayside and nightside reconnection rates, *J. Geophys. Res.*, *112*, A01209, doi:10.1029/2006JA011642.
Milan, S. E., J. Hutchinson, P. D. Boakes, and B. Hubert (2009), Influences on the radius of the auroral oval, *Ann. Geophys.*, *27*, 2913–2924.
Milan, S. E., J. S. Gosling, and B. Hubert (2012), Relationship between interplanetary parameters and the magnetopause reconnection rate quantified from observations of the expanding polar cap, *J. Geophys. Res.*, *117*, A03226, doi:10.1029/2011JA017082.
Morley, S. K., and M. P. Freeman (2007), On the association between northward turnings of the interplanetary magnetic field and substorm onsets, *Geophys. Res. Lett.*, *34*, L08104, doi:10.1029/2006GL028891.
O'Brien, T. P., S. M. Thompson, and R. L. McPherron (2002), Steady magnetospheric convection: Statistical signatures in the solar wind and *AE*, *Geophys. Res. Lett.*, *29*(7), 1130, doi:10.1029/2001GL014641.
Partamies, N., and T. I. Pulkkinen (2009), Different magnetospheric modes: Solar wind driving and coupling efficiency, *Ann. Geophys.*, *27*(11), 4281–4291.
Pulkkinen, T. I., N. Partamies, R. L. McPherron, M. Henderson, G. D. Reeves, M. F. Thomsen, and H. J. Singer (2007), Comparative statistical analysis of storm time activations and sawtooth events, *J. Geophys. Res.*, *112*, A01205, doi:10.1029/2006JA012024.
Pulkkinen, T. I., M. Palmroth, H. E. J. Koskinen, T. V. Laitinen, C. C. Goodrich, V. G. Merkin, and J. G. Lyon (2010), Magnetospheric modes and solar wind energy coupling efficiency, *J. Geophys. Res.*, *115*, A03207, doi:10.1029/2009JA014737.
Sergeev, V. A., R. J. Pellinen, and T. I. Pulkkinen (1996), Steady magnetospheric convection: A review of recent results, *Space Sci. Rev.*, *75*, 551–604.
Shukhtina, M. A., and S. E. Milan, (2014), ECLAT system level data product report (D430.1), *Tech. Rep. 2001*, Univ. of Leicester, Leicester, U. K., doi:10.1007/978-90-481-3499-1.
Wild, J. A., E. E. Woodfield, and S. K. Morley (2009), On the triggering of auroral substorms by northward turnings of the interplanetary magnetic field, *Ann. Geophys.*, *27*, 3559–3570.